PERGAMON

Vision Research 38 (1998) 3591–3599

Vision Research

The effect of suprathreshold contrast on stimulus centroid and its implications for the perceived location of objects

David Whitaker *, Paul V. McGraw

Department of Optometry, University of Bradford, Richmond Road, Bradford, West Yorkshire BD7 1DP, UK

Received 1 July 1997; received in revised form 22 October 1997

Abstract

Using an alignment task, we investigate the role of suprathreshold contrast upon the perceived location of asymmetric Gaussian-windowed stimuli. A model which extracts the centroid of the stimulus envelope between limits defined by contrast threshold accounts well for the observed variation in perceived position. This finding helps to explain previous discrepancies in the literature regarding the validity of stimulus centroid as a determinant of visual location. © 1998 Elsevier Science Ltd. All rights reserved.

Keywords: Localisation; Centroid; Contrast

1. Introduction

Stimulus centroid has long been implicated as the feature which determines the perceived location of luminance-defined objects in the world around us [1–5]. The relevance of centroid analysis was recently extended by Whitaker et al. [6] who showed that contrast-defined objects (Gabor and texture patches) were also perceived as being located at, or close to, the predicted centroid of their contrast envelope. The implication of this finding is that similar, or perhaps identical mechanisms operate on the activity envelope of different types of stimuli prior to the site at which perceptual localisation occurs. Whitaker et al. [6] also examined the effect of suprathreshold contrast level on the relative localisation of asymmetric objects, and present an appreciation of how centroid changes as a function of contrast, although no formal mathematical description of this relationship was provided.

The findings of Whitaker et al. [6] are not consistent with a recent study by Hess and Holliday [7] who used similar stimuli defined by asymmetric luminance and contrast envelopes. The results of the latter study confirm that the perceived location of contrast-defined objects lies close to their centroid, but strongly suggest that luminance-defined objects are located away from their centroid and closer to the peak of the luminance envelope. A possible candidate responsible for the observed discrepancies may be the different levels of suprathreshold contrast employed in the two studies. In the Whitaker et al. [6] study, most of the data were gathered at the maximum contrast affordable by the apparatus. On the other hand, Hess and Holliday [7] used contrasts of 30% for their luminance-defined stimuli and 50% for their stimuli defined by contrast modulation. We now present psychophysical data and a model of how centroid varies with suprathreshold contrast in order to show that contrast is indeed a vital parameter in the localisation of asymmetric stimuli, and must be taken into account in models of centroid analysis.

2. Methods

The methods we used were similar to those used by Whitaker et al. [6] and Hess and Holliday [7] and need only briefly be described here. A three-element alignment task was used in which the horizontal position of the central element had to be judged relative to the outer two elements. The vertical separation between the centres of each element was 2°. The outer two elements were symmetric Gaussian or Gabor patches whilst the

* Corresponding author. Fax: +44 1274 385570; e-mail: d.j.whitaker@bradford.ac.uk.

0042-6989/98/$19.00 © 1998 Elsevier Science Ltd. All rights reserved.
PII: S0042-6989(98)00032-7

central blob was asymmetric, having a different S.D. either side of its peak. The value of this arrangement [7] is that we need only be concerned with the suprathreshold contrast level of the central element, since contrast will not affect the centroid of the outer symmetric elements.

The perceived offset of the central blob was established for a range of asymmetries using a method of constant stimuli. The stimuli were presented within a rectangular temporal window of 500 ms duration. An initial method of adjustment was used to locate the approximate position of perceived alignment thereby allowing efficient positioning of subsequent stimuli. Within any experimental run, perceived offset was established for two stimuli of equal but opposite asymmetry (i.e. one stimulus and its mirror image), and either of these could occur with equal probability on any trial. Each of the two stimuli could be presented at any one of seven offsets, equally spaced around the alignment position suggested by the initial method of adjustment. Step size was either one or two pixels, depending upon the stimulus conditions. Each pixel subtended 1.6 min arc at the viewing distance of 70 cm. During the method of constant stimuli, between 10 and 20 trials were presented at each of the seven offsets, and the proportion of 'rightward' responses was calculated for each offset. Four levels of asymmetry were investigated, defined by the S.D. (in pixels) either side of the peak − 22.8/2.8, 17.8/7.8, 15.3/10.3 and 12.8/12.8 (symmetric). In addition, data were gathered for Gaussian blobs at three levels of Weber contrast ($\Delta L/L_{mean}$) (42, 21 and 10.5%, subject DW; 84, 42 and 21%, subject PVM) and also for Gabor stimuli ($\Delta L_{max}/L_{mean}$) (42, 21 and 10.5% for both subjects). The carrier frequency of the Gabor stimuli was 1.75 cdeg^{-1}.

Contrast detection thresholds for the Gaussian or Gabor blobs at each asymmetry were established using a two-interval forced choice method of constant stimuli. Nine levels of contrast were used, each separated by 0.05 log units. The subject had to decide which one of two 500 ms presentations contained the stimulus. Fifteen presentations were run randomly at each of the nine contrast levels, and bootstrap analysis [8] was used in order to find the contrast resulting in 75% correct response level on the two-interval forced choice psychometric function.

Stimuli were generated using the macro capabilities of the public domain software NIH Image™1.59 (developed at the US National Institutes of Health and available from the Internet by anonymous FTP from zippy.nimh.nih.gov or on floppy disk from the National Technical Information Service, Springfield, VA, part number PB95-500195GEI). Stimuli were presented on a Mitsubishi Diamond Pro 20″ monitor at a mean luminance of 30.1 cd m^{-2} and a frame rate of 75.1 Hz. The non-linear luminance response of the display was linearised using the inverse function of the luminance response as measured with a Minolta CS-100 photometer. Contrast resolution of up to 12-bit accuracy was obtained by combining the red, green and blue outputs of the video board using a video summation device constructed according to Pelli and Zhang [9]. The host computer was a Power Macintosh 7100/80.

The two authors acted as observers, using their dominant eye and having undertaken several practice sessions before data collection began.

3. Results

We adopt the procedure used by Hess and Holliday [7] in which data are presented relative to the pre-calculated centroid for each stimulus. This allows convenient visualisation of the data since, if centroid is indeed the factor determining the perceived localisation of stimuli, data for all levels of asymmetry should collapse together to form a single function. The critical factor represents the method of calculating the centroid. Whitaker et al. [6] have shown that the centroid of an asymmetric Gaussian envelope is given by the simple expression

$$(\sigma_2 - \sigma_1)\sqrt{\frac{2}{\Pi}} \quad (1)$$

(see also Appendix A) where (σ_2-σ_1) represents the difference in S.D. either side of the peak of the envelope. Note that this expression represents the centroid between infinite limits, and assumes that the amplitude of the Gaussian envelope is so great in comparison to threshold that the finite limits defined by threshold can be ignored.

Fig. 1 shows the offset of the central Gaussian blob required to obtain perceptual alignment relative to the centroid of the blob as calculated by Eq. (1). Data for three suprathreshold contrast levels are shown for each observer. Data for each asymmetry level are fitted with a logistic function of the form

$$y = \frac{100}{1 + e^{-\frac{(x-\mu)}{\theta}}}$$

where μ is the offset corresponding to the 50% level on the psychometric function and θ provides an estimate of alignment threshold (half the offset between the 27 and 73% levels on the psychometric function approximately). It is clear from the graphs on the left-hand side of the figure that data for different asymmetries do not collapse together, and this is especially marked at low contrast levels. This represents a clear failure of Eq. (1) to account for the perceived position of the Gaussian elements, and is similar the findings of Hess and Holliday [7] for their 30% contrast Gaussian blobs.

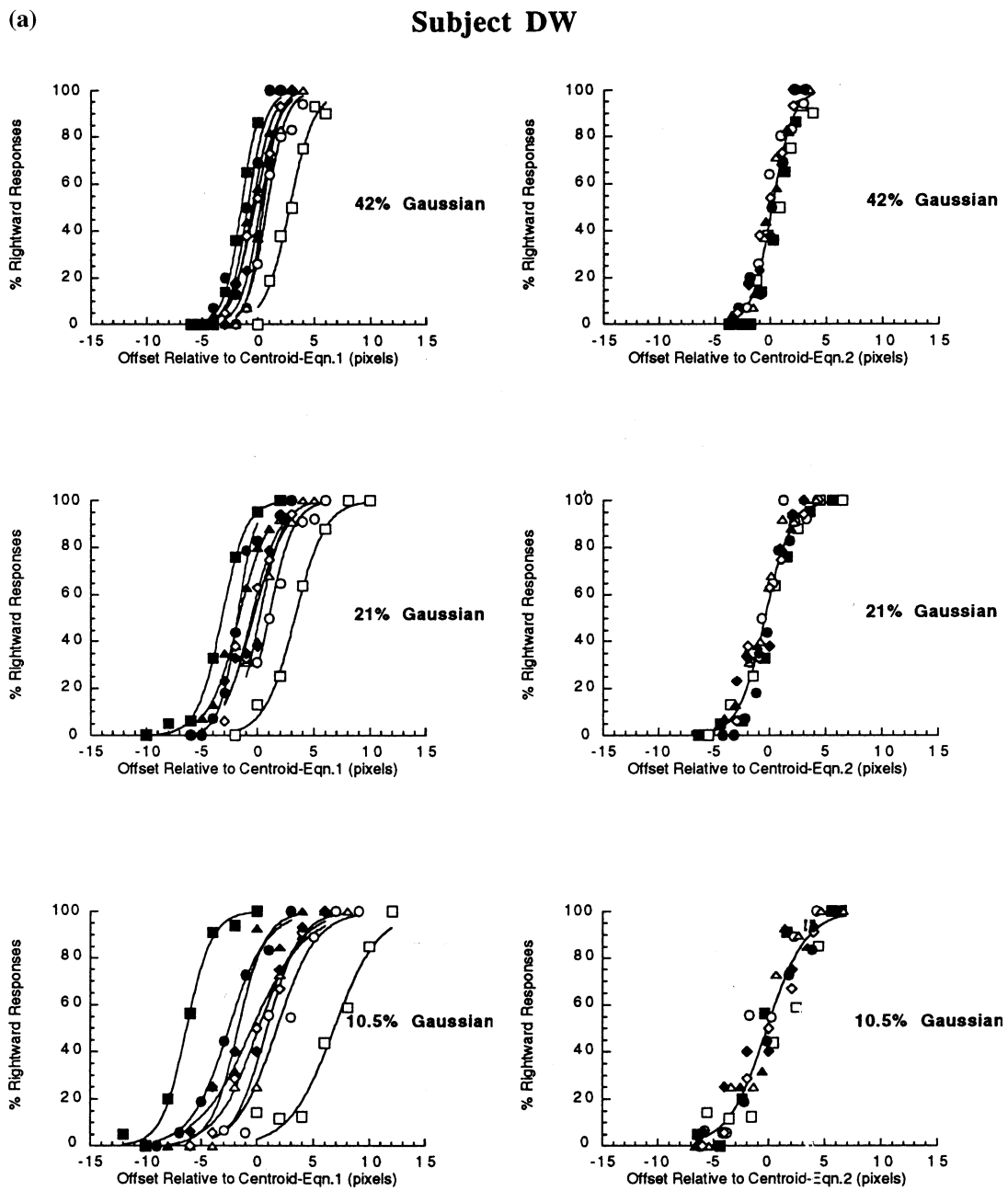

Fig. 1. (a) Subject DW. The left-hand graphs show the percentage of rightward responses plotted against the offset relative to centroid, where the stimulus centroid position is calculated using Eq. (1). Different graphs represent each of three supra-threshold contrast levels. Data sets are shown for Gaussian S.D. of 22.8/2.8 (squares), 17.8/7.8 (circles), 15.3/10.3 (triangles) and 12.8/12.8 (diamonds). The filled and open symbols represent stimuli of equal but opposite polarity of asymmetry. The filled symbols depict stimuli where the centroid is offset to the left of the peak position and the open symbols stimuli where the centroid is offset to the right. Symbol density for the symmetric data was assigned randomly. Each data set has been fitted with a logistic function which is described in the text. The right-hand graphs show corresponding data sets but with the offset position relative to stimulus centroid calculated according to Eq. (2). This has the effect of collapsing all the data from each degree of asymmetry onto a single function, at each supra-threshold contrast level. The entire data set has been fitted with a single logistic function (see text). (b) Gaussian data from subject PVM.

Appendix A provides a mathematical derivation of the centroid of an asymmetric Gaussian when contrast thresholds due to neural noise cannot be considered negligible relative to the amplitude of the Gaussian. In this case, the centroid of the Gaussian needs to be calculated between finite limits, taking threshold into account [6]. We should distinguish here between studies such as the present one which integrate between threshold limits to determine the localisation of the stimulus as a whole and those which are explicitly concerned with threshold limits as determinants of perceived edge location, and hence the perceived size of

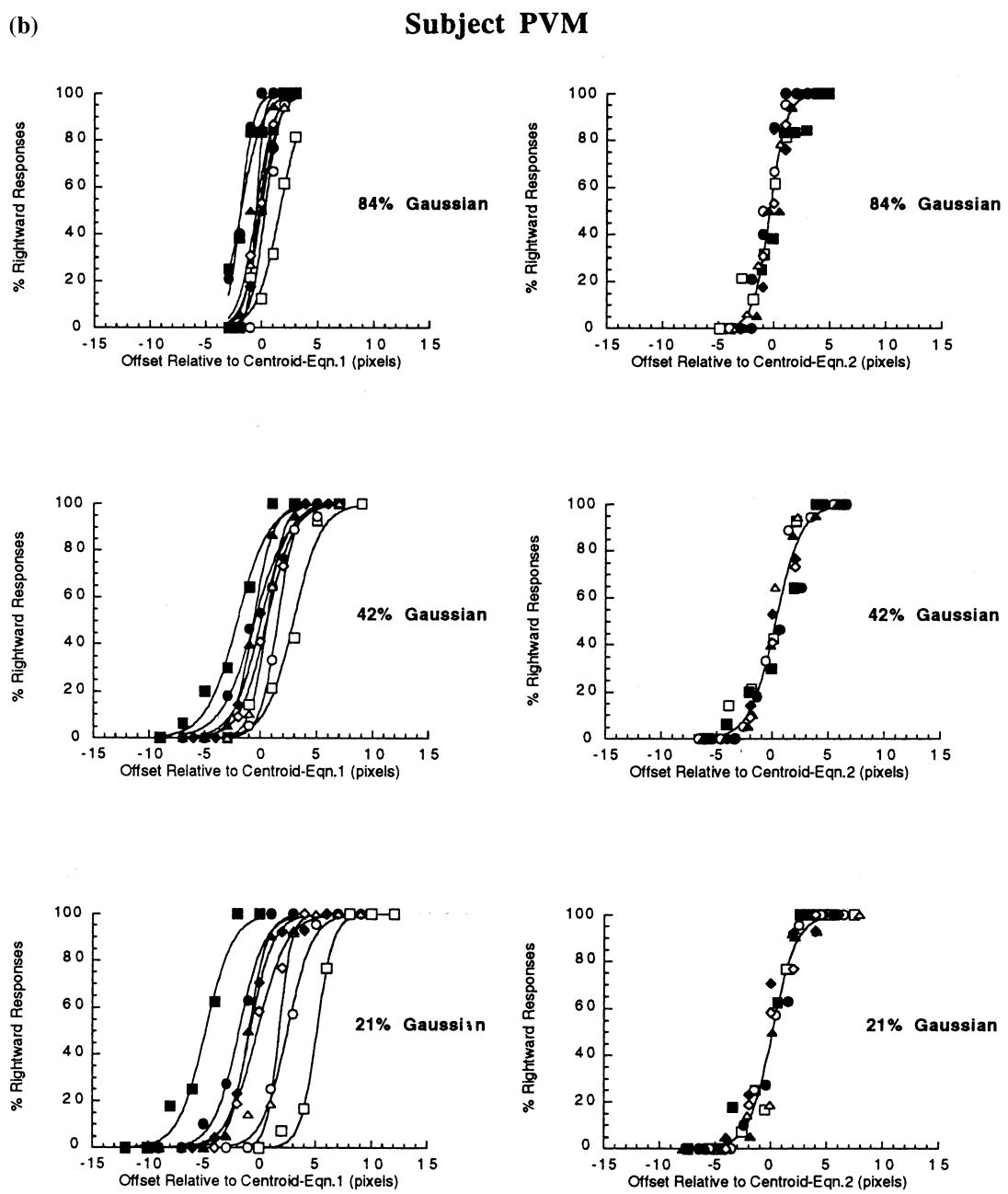

Fig. 1. (*Continued*)

Gaussian-windowed stimuli [10]. Taking threshold limits into account, centroid offset is again proportional to the magnitude of asymmetry, but with a different constant of proportionality:

$$(\sigma_2 - \sigma_1)\frac{\left[(M-1)+\ln\frac{1}{M}\right]}{M\phi\sqrt{\frac{\pi}{2}-\sqrt{-2\ln\frac{1}{M}}}} \quad (2)$$

where M is the multiple of threshold at which the Gaussian is presented and ϕ is a value dependent upon M and found from tables of the cumulative normal distribution as described in Appendix A. When M is very large (i.e. when contrast thresholds are very small relative to the Gaussian amplitude), Eq. (2) reduces to the same form as Eq. (1).

The graphs on the right-hand side of Fig. 1 show the same data as the corresponding graphs on the left, but this time expressed as an offset relative to the centroid of the asymmetric distribution as calculated from Eq. (2). It is clear that, at each contrast level, accounting for contrast thresholds in the centroid calculation provides an excellent description of the data, with data points from all levels of asymmetry collapsing together. The data from all asymmetries are fitted with a single logistic function at each contrast level. Values for the

Table 1
Parameters of the curve fitting procedure for the Gaussian stimuli

	Contrast (%)	$Offset_{50}$ (pixels)	Threshold (pixels)	R^2	χ^2 Eq 2/Eq 1
DW	42	0.13 ± 0.07	0.92 ± 0.06	0.953	0.189
	21	-0.45 ± 0.08	1.18 ± 0.08	0.950	0.188
	10.5	-0.19 ± 0.15	1.74 ± 0.14	0.939	0.137
PVM	84	-0.40 ± 0.07	0.74 ± 0.06	0.946	0.390
	42	0.26 ± 0.09	1.16 ± 0.08	0.974	0.229
	21	0.11 ± 0.09	1.07 ± 0.08	0.970	0.085

Confidence intervals were calculated from the parameter covariance matrix and represent one S.D. either side of the parameter value. χ^2 values for each equation are based upon two degrees of freedom. See text for further details.

offset corresponding to the 50% point of the combined data lie close to zero (see Offset values in Table 1), as would be expected from veridical alignment of the centroid of the middle blob relative to the outer two elements. Thresholds are reduced slightly at the highest contrast for both subjects (see Threshold values in Table 1). The final column of Table 1 provides a quantitative description of the extent to which Eq. (2) accounts for the variance in the data relative to Eq. (1). The value represents a ratio of the residual sum-of-squared deviations from a single logistic fit to the two complete data sets. Values less than one indicate a reduction in variance when suprathreshold contrast level is taken into account by using Eq. (2) rather than Eq. (1).

Equivalent data for the Gabor stimuli are presented in Fig. 2. The data for 10.5% contrast are consistent with those for Gaussian-blob stimuli in that a large proportion of the original variance is accounted for by considering suprathreshold contrast in the model (see Table 2). At 21% there is relatively little variance in the data accounted for by the model which does not consider suprathreshold contrast (Eq. (1)). This is because, at 21% contrast, the Gabor stimuli are already at approximately ten times their contrast detection threshold. Even so, accounting for suprathreshold contrast level further reduces the data variance (see Table 2). At even higher multiples of threshold contrast (42% contrast) Eq. (1) provides a better description of the data than Eq. (2) (see χ^2 ratios above unity in the last column of Table 2). This represents a failure of the suprathreshold contrast model at high multiples of threshold. This is consistent with the findings of Whitaker et al. [6] who also suggest that stimulus-based centroid models do not adequately account for the behaviour of Gabor stimuli at high multiples of threshold contrast.

4. Discussion

Our results show clearly that contrast is an important factor in determining the perceived position of asymmetric Gaussian-windowed stimuli. This is quite consistent with the appearance of asymmetric objects as contrast is varied. At high contrasts the asymmetry is obvious, but becomes less and less pronounced as the contrast of the stimuli approaches threshold. The assumption that Eq. (1) holds across all contrast levels is clearly erroneous, as Whitaker et al. [6] discuss. Proof that this is the case (the present Fig. 1 and Fig. 4 of ref. [7]) is not a failure of centroid analysis, only a failure of an invalid assumption. When threshold is taken into account by using Eq. (2), the data clearly conform closely to what would be expected from assigning perceived position at the centroid of the visible stimulus envelope.

It is important to note that any model such as the one we have adopted is based upon the luminance distribution of the stimulus rather than upon the corresponding internal neural distribution. Therefore, potential non-linearities which may occur between stimulus and the neural response elicited are disregarded. A form of non-linearity might explain the failure of the model for contrast-defined stimuli at high multiples of detection threshold. Appendix B shows the effect that a compressive non-linearity (modelled here in terms of a truncated neural response) would have on centroid location. An example of the effect of a compressive non-linearity has previously been documented for a positional task in the luminance domain by Morgan, et al. [11]. Appendix B demonstrates that Eq. (2) provides a poorer description of the centroid of a truncated stimulus than Eq. (1) at high multiples of threshold contrast, thereby providing a qualitative explanation for the behaviour of the Gabor data at high contrast levels (Fig. 2, 42% contrast). A quantitative account of the data would simply require an appropriate choice of non-linearity.

Knowledge of the important role of contrast in determining the perceived location of asymmetric stimuli allows some important insights into the success or otherwise of previous studies to produce data conforming to centroid behaviour. The studies which support a centroid-based strategy have used bright, localised line stimuli on dark backgrounds [1,5,12,13] or high-density

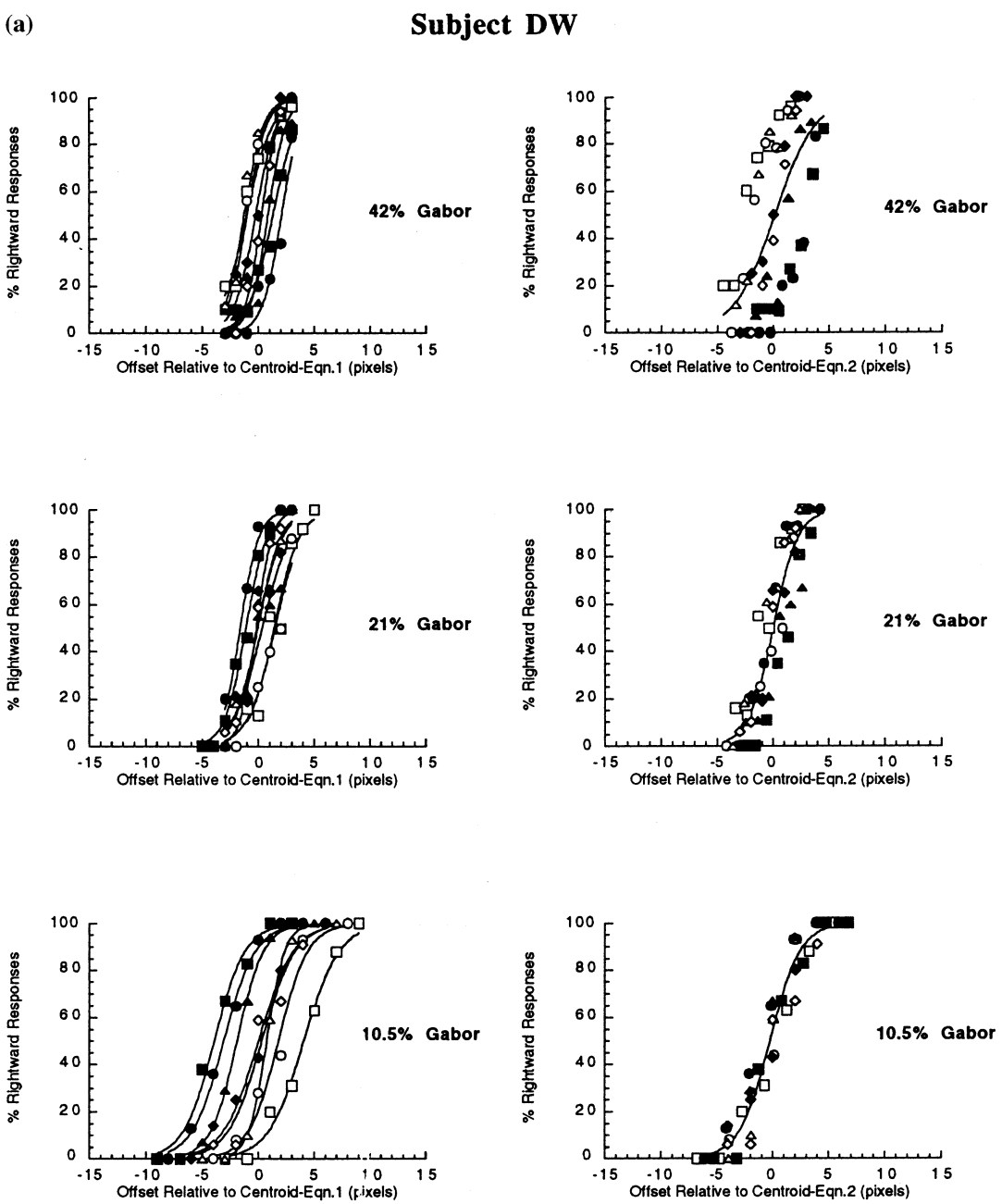

Fig. 2. (a) Subject DW. As for Fig. 1, but for Gabor stimuli at three suprathreshold contrast levels. Use of Eq. (2) (right-hand graphs) has the effect of collapsing all the data from each degree of asymmetry onto a single function at low supra-threshold contrast levels. However, at the highest contrast, application of Eq. (2) leads to a slight increase in variance of the data. (b) Gabor data from subject PVM.

clusters of bright dots against a dark background [3]. Low contrast stimuli have resulted in problems for models of centroid analysis, as Hess and Holliday [7] observed. Both Whitaker and Walker [3] and Whitaker and MacVeigh [14], using asymmetric clusters of bright dots, found that their data conformed well to a model based upon centroid only when dot density was high. At low dot densities, the perceived contrast of the clusters was much lower, and the centroid model failed. Low dot density patterns were also used by Ward et al. [15] leading them to conclude that a localisation strategy based upon stimulus centroid was inappropriate.

In summary, we have examined the effect of suprathreshold contrast on the perceived location of asymmetric stimuli. The data are consistent with a localisation strategy based upon stimulus centroid provided appropriate consideration is given to the level of suprathreshold contrast. This analysis helps to explain discrepancies between previous studies

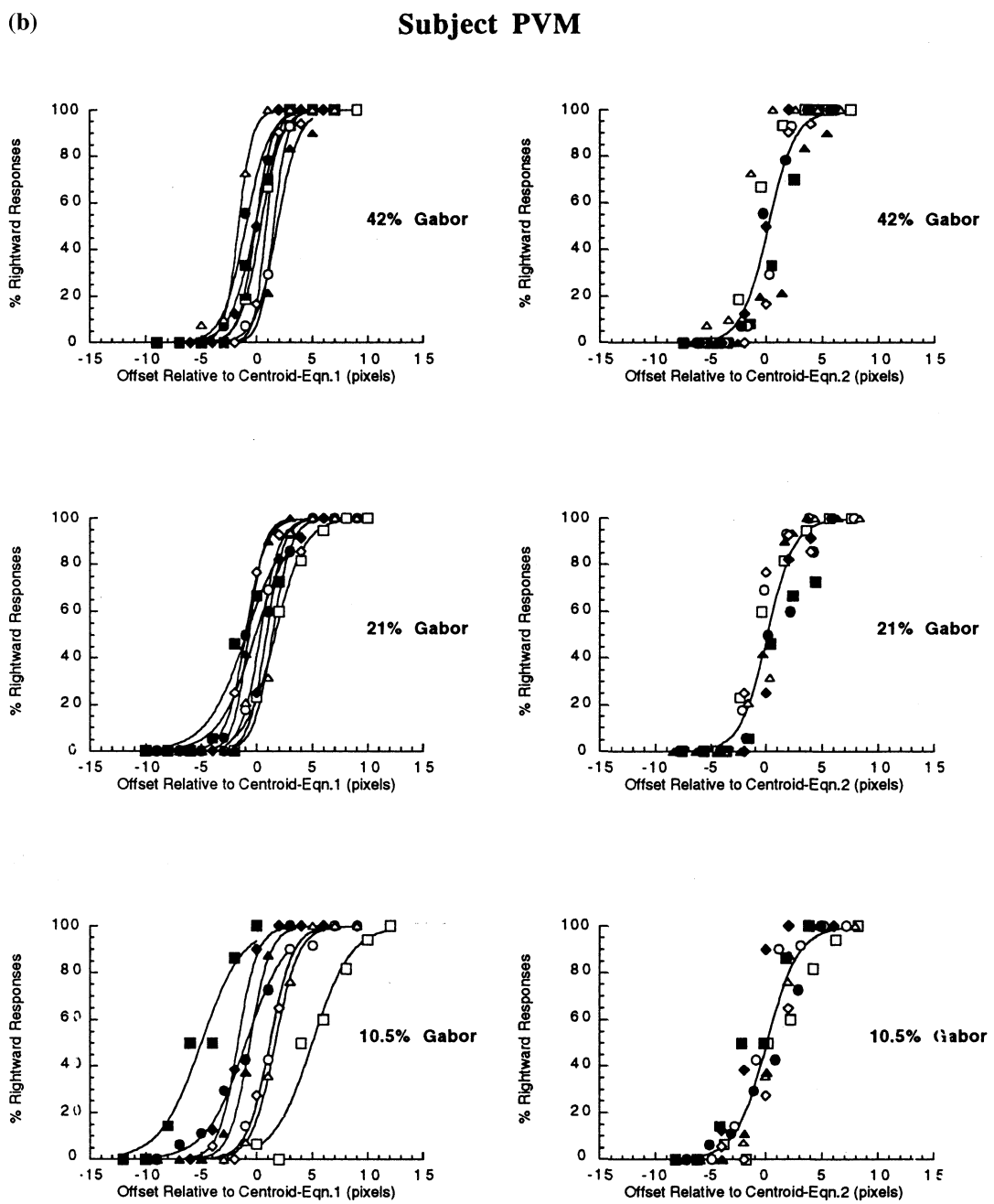

Fig. 2. (*Continued*)

Table 2
Parameters of the curve fitting procedure for the Gabor stimuli

	Contrast (%)	$Offset_{50}$ (pixels)	Threshold (pixels)	R^2	χ^2 Eq 2/Eq 1
DW	42	0.12 ± 0.34	1.84 ± 0.38	0.455	2.16
	21	-0.01 ± 0.12	1.11 ± 0.11	0.868	0.624
	10.5	-0.27 ± 0.10	1.36 ± 0.09	0.968	0.115
PVM	42	0.18 ± 0.21	1.22 ± 0.18	0.881	1.25
	21	0.10 ± 0.15	1.21 ± 0.13	0.934	0.835
	10.5	0.07 ± 0.18	1.42 ± 0.16	0.913	0.279

Confidence intervals were calculated from the parameter covariance matrix and represent one S.D. either side of the parameter value. χ^2 values for each equation are based upon two degrees of freedom. See text for further details.

which have examined the role of stimulus centroid in models of localisation.

Acknowledgements

P.V. McGraw is supported by a Vision Research Training Fellowship from the Wellcome Trust. Additional support was provided by the Visual Research Trust. We are grateful to R. Hess for helpful comments on an earlier draft of this manuscript.

Appendix A. Finding the centroid of an asymmetric Gaussian above a threshold level T

The centroid of an asymmetric Gaussian profile having S.D. σ_1 and σ_2 either side of the peak is given by

$$\frac{\int_{-\infty}^{\infty} xy\ dx}{\int_{-\infty}^{\infty} y\ dx} = \frac{-\sigma_1^2\left[1-\exp\left(\frac{-\infty^2}{2\sigma_1^2}\right)\right]-\sigma_2^2\left[\exp\left(\frac{-\infty^2}{2\sigma_2^2}\right)-1\right]}{\sigma_1\sqrt{\frac{\Pi}{2}}+\sigma_2\sqrt{\frac{\Pi}{2}}}$$

(Appendix 1 of ref. [6]). This simplifies to

$$(\sigma_2-\sigma_1)\sqrt{\frac{2}{\Pi}} \tag{A1}$$

The present Appendix finds an expression for the centroid of an asymmetric Gaussian when the limits are not assumed to be infinite. The Figure below shows an asymmetric Gaussian profile with an amplitude represented by a given multiple, M of threshold, T.

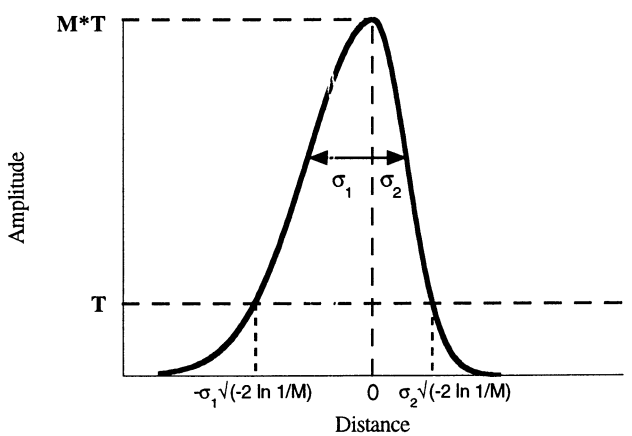

The distance from the peak of the Gaussian at which the amplitude falls to $1/M$ of its maximum is given by:

$$T = M*T\ \exp\left(\frac{-x^2}{2\sigma^2}\right)$$

Hence,

$$x = \sigma\sqrt{-2\ln\frac{1}{M}}$$

The centroid of the area within these limits and above threshold, T, is therefore given by

$$\frac{\int_{-\sigma_1\sqrt{-2\ln(1/M)}}^{\sigma_2\sqrt{-2\ln(1/M)}} x\left(y-\frac{1}{M}\right)\ \mathrm{d}x}{\int_{-\sigma_1\sqrt{-2\ln(1/M)}}^{\sigma_2\sqrt{-2\ln(1/M)}}\left(y-\frac{1}{M}\right)\ \mathrm{d}x}$$

which equals:

$$\frac{-\sigma_1^2\left[1-\exp\left(\frac{\sigma_1^2 2\ln\left(\frac{1}{M}\right)}{2\sigma_1^2}\right)\right]-\sigma_2^2\left[\exp\left(\frac{\sigma_2^2 2\ln\left(\frac{1}{M}\right)}{2\sigma_2^2}\right)-1\right]-\int_{-\sigma_1\sqrt{-2\ln(1/M)}}^{\sigma_2\sqrt{-2\ln(1/M)}}\frac{x}{M}\ \mathrm{d}x}{\int_{-\sigma_1\sqrt{-2\ln(1/M)}}^{0}\exp\left(\frac{-x^2}{2\sigma_1^2}\right)\ \mathrm{d}x+\int_{0}^{\sigma_2\sqrt{-2\ln(1/M)}}\exp\left(\frac{-x^2}{2\sigma_2^2}\right)\ \mathrm{d}x-\int_{-\sigma_1\sqrt{-2\ln(1/M)}}^{\sigma_2\sqrt{-2\ln(1/M)}}\frac{1}{M}dx}$$

Expanding:

$$\frac{\left[(\sigma_2^2-\sigma_1^2)\left(1-\frac{1}{M}\right)\right]-\left[\frac{1}{2M}\left((\sigma_2^2-\sigma_1^2)\left(-2\ln\left(\frac{1}{M}\right)\right)\right)\right]}{\phi\sigma_1\sqrt{\frac{\Pi}{2}}+\phi\sigma_2\sqrt{\frac{\Pi}{2}}-\left[\left(\frac{1}{M}\right)(\sigma_1+\sigma_2)\left(\sqrt{-2\ln\frac{1}{M}}\right)\right]}$$

where $(0<\phi<1)$ is a value representing the cumulative distribution function of the standard normal distribution between the limits of the relevant integral. The true value of ϕ is given by an infinite alternating series, so it is easiest to find its value from tables of the cumulative normal distribution which can be found in almost every textbook on statistics. The above expression simplifies to:

$$(\sigma_2-\sigma_1)\frac{\left[(M-1)+\ln\frac{1}{M}\right]}{M\phi\sqrt{\frac{\pi}{2}}-\sqrt{-2\ln\frac{1}{M}}} \tag{A2}$$

Thus, when M is very large, $\phi\to 1$ and the equation reduces to Eq. (A1). As $M\to 1$, i.e. the amplitude of the Gaussian is close to threshold, the centroid converges to zero.

Appendix B. Finding the centroid of a truncated asymmetric Gaussian above a threshold level *T*

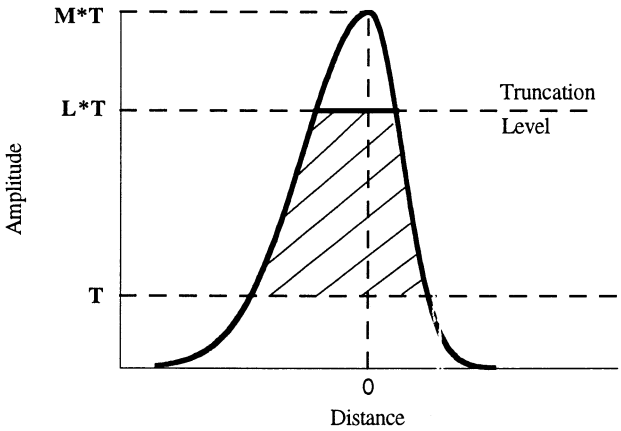

The centroid of an asymmetric Gaussian above a threshold level, T, and which is truncated at a multiple L times threshold (hatched area) is given by

$$\frac{\int_{-\sigma_1\sqrt{-2\ln(1/M)}}^{\sigma_2\sqrt{-2\ln(1/M)}} x\left(y-\frac{1}{M}\right)\,dx-\int_{-\sigma_1\sqrt{-2\ln(L/M)}}^{\sigma_2\sqrt{-2\ln(L/M)}} x\left(y-\frac{L}{M}\right)\,dx}{\int_{-\sigma_1\sqrt{-2\ln(1/M)}}^{\sigma_2\sqrt{-2\ln(1/M)}}\left(y-\frac{1}{M}\right)\,dx-\int_{-\sigma_1\sqrt{-2\ln(L/M)}}^{\sigma_2\sqrt{-2\ln(L/M)}}\left(y-\frac{L}{M}\right)\,dx}$$

Expanding as in Appendix A and simplifying, we end up with the expression

$$(\sigma_2-\sigma_1)\frac{(L-1)+\left[(1-L)\ln\left(\frac{1}{M}\right)\right]+\left[L\ln\left(\frac{1}{L}\right)\right]}{\left[M(\phi_1-\phi_2)\sqrt{\frac{\pi}{2}}\right]-\sqrt{-2\ln\left(\frac{1}{M}\right)}+\left[L\sqrt{-2\ln\left(\frac{L}{M}\right)}\right]} \qquad \text{(A3)}$$

where ϕ_1 and ϕ_2 are values representing the cumulative distribution function of the standard normal distribution between limits defined by the threshold level and truncation level respectively. As $L \to M$, Eq. (A3) reduces to Eq. (A2). The figure below shows the behaviour of Eqs. (A1), (A2) and (A3) as a function of multiple of threshold contrast, M. At low multiples of threshold contrast, Eqs. (A1) and (A2) diverge, which explains why Eq. (A1) (which takes no account of suprathreshold contrast) fails to predict performance at low levels of stimulus contrast (Figs. 1 and 2). Comparison of Eqs. (A3) and (A2) indicates that a compressive non-linearity at high contrasts (modelled here in terms of a truncated neural response) can result in an elevation of centroid offset beyond that predicted by Eq. (A2) and even Eq. (A1). This may explain the failure of both equations (particularly Eq. (A2)) to predict performance for the high contrast Gabor stimuli (Fig. 2).

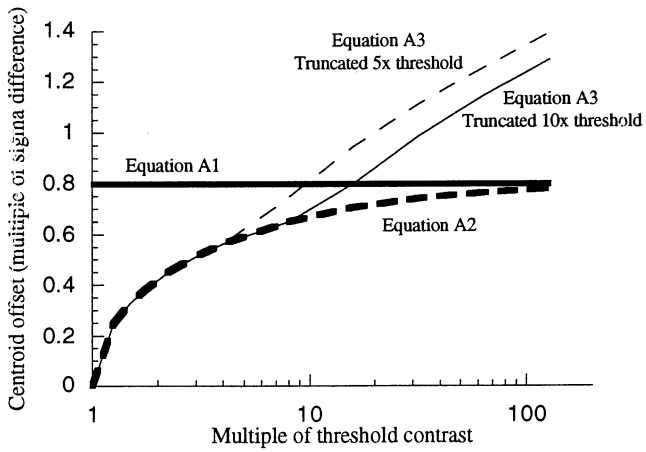

References

[1] Westheimer G, McKee SP. Integration regions for visual hyperacuity. Vis Res 1977;17:89–93.
[2] Watt RJ, Morgan MJ, Ward RM. Stimulus features that determine the visual location of a bright bar. Invest Ophthalmol Vis Sci 1983;24:66–71.
[3] Whitaker D, Walker H. Centroid evaluation in the Vernier alignment of random dot clusters. Vis Res 1988;28:777–84.
[4] Hirsch J, Mjolsness E. A centre-of-mass computation describes the precision of random dot displacement discrimination. Vis Res 1992;32:335–46.
[5] Morgan MJ, Ward RM, Cleary RF. Motion displacement thresholds for compound stimuli predicted by the displacement of centroids. Vis Res 1994;34:747–9.
[6] Whitaker D, McGraw PV, Pacey I, Barrett BT. Centroid analysis predicts visual localization of first- and second-order stimuli. Vis Res 1996;36:2957–70.
[7] Hess RF, Holliday I. Primitives used in the spatial localization of non-abutting stimuli: peaks or centroids. Vis Res 1996;36:3821–6.
[8] Foster DH, Bischof WF. Thresholds from psychometric functions: superiority of bootstrap to incremental and probit variance estimates. Psychol Bull 1991;109:152–9.
[9] Pelli DG, Zhang L. Accurate control of contrast on microcomputer displays. Vis Res 1991;31:1337–50.
[10] Fredericksen RE, Bex PJ, Verstraten FAJ. How big is a Gabor patch, and why should we care? J Opt Soc Am A 1997;14:1–12.
[11] Morgan MJ, Mather G, Moulden B, Watt RJ. Intensity-response non-linearities and the theory of edge localization. Vis Res 1984;24:713–9.
[12] Watt RJ, Morgan MJ. Mechanisms responsible for the assessment of visual location: theory and evidence. Vis Res 1983;23:97–109.
[13] Levi DM, Westheimer G. Spatial-interval discrimination in the human fovea: what delimits the interval? J Opt Soc Am A 1987;4:1304–13.
[14] Whitaker D, MacVeigh D. Sequential mapping of weighting functions for visual location. Spat Vis 1992;6:117–31.
[15] Ward RM, Casco C, Watt RJ. The location of noisy visual stimuli. Can J Psychol 1985;39:387–99.